The Journal of Immunology

Cutting Edge: Elevated Glycolytic Metabolism Limits the Formation of Memory CD8 $^{+}$ T Cells in Early Life

Cybelle Tabilas, Jocelyn Wang, Xiaojing Liu, Jason W. Locasale, Norah L. Smith and Brian D. Rudd

J Immunol 2019; 203:2571-2576; Prepublished online 9 October 2019;
doi: 10.4049/jimmunol.1900426
http://www.jimmunol.org/content/203/10/2571

The Journal of Immunology is published twice each month by
The American Association of Immunologists, Inc.,
1451 Rockville Pike, Suite 650, Rockville, MD 20852

Print ISSN: 0022-1767 Online ISSN: 1550-6606.

Cutting Edge

The Journal of Immunology

Cutting Edge: Elevated Glycolytic Metabolism Limits the Formation of Memory CD8$^+$ T Cells in Early Life

Cybelle Tabilas,*[,1] Jocelyn Wang,[†,1] Xiaojing Liu,[‡] Jason W. Locasale,[§] Norah L. Smith,* and Brian D. Rudd*

Neonates often develop poor immunity against intracellular pathogens. Because CD8$^+$ T cells are essential for eliminating infectious agents, it is crucial to understand why they behave differently in early life. Previous studies in mice have demonstrated that neonatal CD8$^+$ T cells fail to form memory because of an intrinsic propensity to differentiate into short-lived effectors. However, the underlying mechanisms remain undefined. We now show that neonatal CD8$^+$ T cells exhibit higher glycolytic activity than adult CD8$^+$ T cells postinfection, which may be due to age-related differences in Lin28b expression. Importantly, when glycolysis is pharmacologically inhibited, the impaired formation of neonatal memory CD8$^+$ T cells can be restored. Collectively, these data suggest that neonatal CD8$^+$ T cells are inherently biased toward undergoing glycolytic metabolism postinfection, which compromises their ability to develop into memory CD8$^+$ T cells in early life. *The Journal of Immunology*, **2019, 203: 2571–2576.**

Infections remain a major cause of neonatal morbidity and mortality. Repeated infections with the same intracellular pathogen (respiratory syncytial virus, rhinovirus) are common in early life (1), indicating a reduced capacity to develop neonatal memory CD8$^+$ T cells. However, the basic mechanisms that prevent neonates from generating robust memory CD8$^+$ T cell responses are poorly understood, and the lack of this knowledge has limited our ability to develop more rational strategies to enhance immunity in early life.

During infection, naive Ag-specific CD8$^+$ T cells undergo massive clonal expansion and differentiate into effector CD8$^+$ T cells capable of eliminating infected cells (2–4). Once the infection has been controlled, the majority (~90–95%) of CD8$^+$ T cells undergo apoptosis. However, a small percentage (~5–10%) of cells survive and differentiate into long-lived memory cells, protecting the host against reinfection. Recent studies have demonstrated that neonatal CD8$^+$ T cells are intrinsically defective at forming memory CD8$^+$ T cells (5–7). Surprisingly, this impairment is not due to a lack of responsiveness or proliferation but rather to an inherent propensity of neonatal CD8$^+$ T cells to rapidly become terminally differentiated, thereby losing their potential to transition into the long-lived memory pool (7).

The propensity for CD8$^+$ T cells to become terminally differentiated in early life relates to the unique properties of the hematopoietic stem cells (HSCs) from which neonatal CD8$^+$ T cells are derived (8). Whereas neonatal CD8$^+$ T cells are produced from highly proliferative fetal HSCs that originate in the liver (9, 10), adult CD8$^+$ T cells are generated from more quiescent adult HSCs in the bone marrow (9, 11). Notably, fetal HSCs use distinct metabolic pathways compared with adult HSCs, which are largely regulated by Lin28b (12–14). Lin28b is a classic oncofetal gene that creates a metabolic program conducive for rapid cell growth in fetal life as well as in aggressive cancers (15). Whether this metabolic program is retained in neonatal CD8$^+$ T cells and alters their fate during infection remains an open question.

In adults, CD8$^+$ T cells undergo extensive changes in their metabolic properties throughout the course of infection. Following activation, naive CD8$^+$ T cells switch their glucose metabolism from oxidative phosphorylation to aerobic glycolysis, similar to cancer cells (16–18). This phenomenon (known as the Warburg effect) is required to mobilize sufficient amounts of proteins, nucleic acids, lipids, and carbohydrates to undergo massive clonal expansion (19) and acquire effector functions (20). Once the infection has been cleared, effector CD8$^+$ T cells must decrease anabolic activity to become more quiescent memory cells. This is accomplished by switching from glycolysis back to fatty acid oxidation (21–23). In this study, we investigated whether age-related differences in metabolic programming underlie the impaired development of neonatal memory CD8$^+$ T cells.

*Department of Microbiology and Immunology, Cornell University, Ithaca, NY 14853; [†]Department of Pediatrics, Indiana University, Indianapolis, IN 46202; [‡]Department of Molecular and Structural Biochemistry, North Carolina State University, Raleigh, NC 27695; and [§]Department of Pharmacology and Cancer Biology, Duke University, Durham, NC 27710

[1]C.T. and J.W. contributed equally to this work.

ORCIDs: 0000-0001-5846-7269 (C.T.); 0000-0003-0016-3136 (J.W.); 0000-0002-4231-6017 (X.L.); 0000-0002-7766-3502 (J.W.L.).

Received for publication April 15, 2019. Accepted for publication September 20, 2019.

This work was supported by National Institutes of Health/National Institute of Allergy and Infectious Diseases Grants R01AI105265 and R01AI110613 (to B.D.R.) and National Institutes of Health/National Institute of Biomedical Imaging and Bioengineering T32 Training Grant 1T32EB023860 (to C.T.).

Address correspondence and reprint requests to Dr. Brian D. Rudd, Department of Microbiology and Immunology, Cornell University, C5 147 VMC, Ithaca, NY 14853. E-mail: bdr54@cornell.edu

The online version of this article contains supplemental material.

Abbreviations used in this article: 2-DG, 2-deoxy-D-glucuse; dpi, day postinfection; ECAR, extracellular acidification rate; HSC, hematopoietic stem cell; Lin28b Tg, Lin28b transgenic; LM-gB, *Listeria monocytogenes* expressing the gB-8p peptide; MPEC, memory precursor cell; OCR, oxygen consumption rate; qPCR, quantitative PCR; SLEC, short-lived effector cell; SRC, spare respiratory capacity; TN, true naive; VM, virtual memory; WT, wild-type.

www.jimmunol.org/cgi/doi/10.4049/jimmunol.1900426

Materials and Methods

Mice

B6-Ly5.2/Cr mice were purchased from Charles River Laboratories. TCR transgenic mice specific for the HSV-1 glycoprotein $gB_{498–505}$ peptide SSIEFARL [gBT-I mice (24)] were provided by J. Nikolich-Zugich (University of Arizona, Tucson, AZ) and crossed with Thy1.1 or C57BL/6 mice purchased from The Jackson Laboratory. Lin28b transgenic (Lin28b Tg) mice (25) driven under the CD2 promoter were provided by L. Pobezinsky (University of Massachusetts) and crossed with gBT-I mice. Neonatal and adult gBT-I animals of both sexes were used at 5–7-d and 2–4-mo-old, respectively. Mice were housed under specific pathogen–free conditions at Cornell University College of Veterinary Medicine, accredited by the Assessment and Accreditation of Laboratory Animal Care.

In vitro T cell stimulation assays

Splenic $CD8^+$ T cells were isolated from gBT-I mice by positive immunomagnetic selection (Miltenyi Biotec), stimulated with plate-bound anti-CD3 (5 μg/ml) and anti-CD28 (20 μg/ml), and cultured in complete media supplemented with 10 U/ml IL-2 (BioLegend) for 48 h. For glycolytic inhibition experiments, cells were cultured with media supplemented with 0.3 mM 2-deoxy-D-glucuse (2-DG; Sigma-Aldrich).

Dual adoptive transfer experiments

gBT-I splenic neonatal and adult $CD8^+$ T cells were enriched by positive immunomagnetic selection (Miltenyi Biotec). Combined cells were suspended at 5×10^5 cells/ml of PBS and 100 μl was injected i.v. into adult B6-CD45.1 recipient mice. The next day, recipient mice were infected (5×10^3 CFU, i.v.) with wild-type (WT) *Listeria monocytogenes* expressing the gB-8p peptide (LM-gB), as previously described (6).

Abs and flow cytofluorimetric analysis

Abs were purchased from eBioscience, BioLegend, Invitrogen, or BD Biosciences, and concentrations were used as recommended by the manufacturer. Flow cytofluorimetric data were acquired using FACSDiva software from an LSRII equipped with four lasers (BD Biosciences). Analysis was performed with FlowJo (Tree Star, Ashland, OR).

Cell sorting

To perform metabolic flux analysis, donor $CD8^+$ T cells were recovered from recipient mice by positive immunomagnetic selection (Miltenyi Biotec) and subsequently labeled with Abs against CD8 (53-6.7), CD4 (Gk1.5), CD45.1 (A20), CD45.2 (104), and Thy1.1 (OX-7). For experiments that isolated true naive (TN) and virtual memory (VM) populations, Abs against CD122 (Tm-b1) and CD44 (IM7) were used. For experiments that isolated the short-lived effector cell (SLEC) population, Abs against KLRG1 (2F1) and CD127 (A7R34) were used. The cells were then sorted to >95% purity on a FACSAria III (BD Biosciences).

Metabolic bioassays

To measure oxygen consumption rates (OCR) and extracellular acidification rates (ECAR), $2.5–3\times10^5$ sorted $CD8^+$ T cells were plated in buffer-free media containing 2 mM glutamine and 1 mM sodium pyruvate. Twenty-five millimolars glucose was additionally supplemented to measure OCR. Using a Seahorse XFp Extracellular Flux Analyzer (Agilent, Santa Clara, CA), OCR was measured following the addition of 1 μM oligomycin, 1 μM FCCP, and 0.5 μM rotenone/antimycin A, and ECAR was measured following the addition of 10 mM glucose, 1 μM oligomycin, and 50 μM 2-DG.

Quantitative PCR

RNA was isolated using TRIzol (Life Technologies), and cDNA was generated with the iScript Reverse Transcription Supermix kit (Bio-Rad). Real-time RT-PCR was performed on an Applied Biosystems 7900HT with primers that have been previously described (26). Gene expression was calculated relative to Actb.

Metabolomics

Metabolite extraction from activated neonatal and adult $CD8^+$ T cells was performed exactly as described in a previous study (27). An liquid chromatography-mass spectrometry (Q Exactive mass spectrometer; Thermo Fisher Scientific) was used for metabolite profiling, and the relative abundance of each metabolite was calculated using the commercially available software Sieve 2.2 (Thermo Fisher Scientific) according to previously described procedures (27).

Statistical analysis

Statistical analysis was performed using Prism (GraphPad Software, La Jolla, CA). Error bars represent SEM and are representative of biological replicates within an experiment. Significance was determined by Student *t* test or a two-way ANOVA followed by a Tukey post hoc test as indicated in the figure legends. The *p* values <0.05 were considered significant.

Results and Discussion

Neonatal $CD8^+$ T cells exhibit higher glycolytic metabolism after in vitro stimulation

Previous studies have demonstrated that neonatal T cells from mice (6–8, 28, 29) and humans (7, 30, 31) are inherently more reactive than their adult counterparts after in vitro stimulation. To understand the metabolic changes that occur during this process, we activated $CD8^+$ T cells from neonatal and adult TCR transgenic mice (gBT-I mice) and used the Seahorse Extracellular Flux Analyzer to compare their bioenergetics profiles. After 2 d of stimulation via the TCR and CD28, we found that the basal OCR, an indicator of oxidative phosphorylation, was higher in adult cells (Fig. 1A, 1B). In contrast, neonatal $CD8^+$ T cells exhibited a higher basal ECAR (Fig. 1C), which is used as a readout for aerobic glycolysis. Overall, neonatal $CD8^+$ T cells possessed a lower OCR/ECAR ratio (Fig. 1D), suggesting that $CD8^+$ T cells in early life preferentially use glycolytic metabolism poststimulation.

To extend our extracellular flux data, we performed quantitative PCR (qPCR) and compared the expression levels of genes in the glycolysis pathway in neonatal and adult $CD8^+$ T cells at 8 h poststimulation. We found that most of the key genes involved in glycolysis were highly upregulated in neonatal $CD8^+$ T cells after activation (Fig. 1F). We also used liquid chromatography/high-resolution mass spectrometry to determine how glycolytic metabolites are altered in different-aged $CD8^+$ T cells at 18 h poststimulation. In line with our qPCR data, neonatal $CD8^+$ T cells produced higher amounts of metabolites involved in the glycolysis pathway (e.g., pyruvate, lactate) than adults (Supplemental Fig. 1). Collectively, these findings demonstrate that neonatal $CD8^+$ T cells undergo augmented glycolysis following TCR activation.

Neonatal $CD8^+$ T cells possess an inherent propensity to undergo glycolytic metabolism following infection

We next assessed the metabolic changes that occur in neonatal and adult $CD8^+$ T cells postinfection in vivo. Our strategy was to cotransfer the same number of neonatal (Thy1.2) and adult (Thy1.1) gBT-I TCR transgenic cells into congenic recipients (Ly5.2 mice), which were subsequently infected with recombinant LM-gB (Fig. 2A). By comparing equal numbers of monoclonal neonatal and adult $CD8^+$ T cells in the same environment, we were able to focus on cell-intrinsic differences in metabolic reprogramming. Consistent with our earlier work (6), neonatal $CD8^+$ T cells preferentially gave rise to SLECs ($KLRG1^+$, $CD127^-$), whereas adult $CD8^+$ T cells formed more memory precursor cells (MPECs; $KLRG1^-$, $CD127^+$) postinfection (Fig. 2B). To compare their metabolic profiles, we used FACS to isolate neonatal and adult donor cells at the peak of infection (7 d postinfection [dpi]) and performed extracellular flux analysis under basal conditions and after drug-induced stress. Neonatal donor $CD8^+$ T cells exhibited a lower basal and maximum OCR and a higher basal and maximum ECAR compared with their adult counterparts (Fig. 2C, 2D). Moreover, neonatal $CD8^+$ T cells

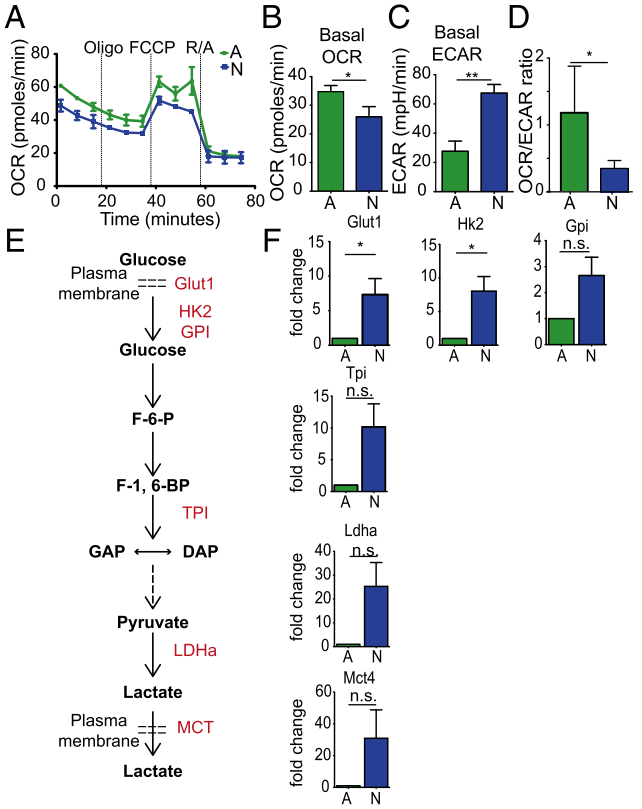

FIGURE 1. Neonatal CD8$^+$ T cells exhibit higher glycolytic metabolism after in vitro stimulation. (**A**) OCR measurements of adult and neonatal CD8$^+$ T cells at 48 h after anti-CD3 and anti-CD28 activation. (**B**) Basal OCR, (**C**) basal ECAR, and (**D**) basal OCR/ECAR ratios in adult and neonatal CD8$^+$ T cells at 48 h after anti-CD3 and anti-CD28 activation. (**E**) Pathway of critical proteins in glycolysis. (**F**) Fold change in mRNA expression of proteins 8 h poststimulation using qPCR. Data representative of two independent experiments with three to five biological replicates per group. $^*p < 0.05$, $^{**}p < 0.005$ by unpaired Student *t* test.

had significantly lower levels of spare respiratory capacity (SRC) (Fig. 2E), which has previously been shown to be critical for the development of memory CD8$^+$ T cells (32). These results suggest that neonatal CD8$^+$ T cells fail to transition into the long-lived memory pool because of an inability to undergo oxidative metabolism in response to increased stress.

To better understand why neonatal CD8$^+$ T cells use different metabolic programs than adults postinfection, we next performed a series of experiments to control for phenotypic differences that are present before and postinfection. First, we considered that age-related changes in metabolic reprogramming might be due to differences in the proportion of naive and VM cells in the starting pool. Indeed, we previously found that neonatal CD8$^+$ T cells comprise nearly twice as many VM cells (Ag-inexperienced cells with a memory phenotype) as adults prior to infection (8). To control for these initial phenotypic differences, we repeated our cotransfer experiments with sorted populations of CD44^{lo}CD122^{lo} TN and CD44^{hi}CD122^{hi} VM donor cells from neonatal and adult gBT-I mice and directly compared their metabolic profiles at the peak of infection (Supplemental Fig. 2A, 2B). Regardless of the initial phenotype, the neonatal donor cells (both TN and VM) use an elevated glycolytic program compared with their adult counterparts (Supplemental Fig. 2C–G). These data suggest that age-related changes in metabolic reprogramming cannot be simply explained by the different phenotypes of cells that are present prior to infection.

Second, we tested the possibility that metabolic changes observed in neonatal and adult effector CD8$^+$ T cells are due to phenotypic differences that are present at the peak of the response. For example, the lower levels of OCR and SRC observed in neonatal cells could be due to a higher proportion of SLECs in the bulk population rather than a difference in metabolic programming in the responding cells. To examine this possibility, we repeated our cotransfer experiment. However, this time we sorted out an equivalent phenotypic subset (SLECs) from neonatal and adult donor cells at the peak of the response (7 dpi) and directly compared their metabolic profiles (Supplemental Fig. 2H). The adult SLECs still showed higher rates of basal and maximum OCR and exhibited a larger SRC compared with neonatal SLECs (Supplemental Fig. 2I–K). In contrast, the neonatal SLECs displayed higher basal and maximum ECAR (Supplemental Fig. 2L, 2M), which is consistent with the overall metabolic programs observed in the bulk neonatal and adult populations. Taken together, these data suggest that age-related differences in metabolic reprogramming of CD8$^+$ T cells are due to inherent changes at the individual cell level rather than shifts in the representation of naive or effector subsets in the mixed population.

Lin28b drives a more glycolytic metabolic program in CD8$^+$ T cells

Another key question is, how are neonatal CD8$^+$ T cells programmed to use glycolysis postinfection? We previously showed that neonatal and adult CD8$^+$ T cells adopt different fates during infection because they are derived from distinct progenitor populations, which are specified, at least in part, by their differential expression of Lin28b (8). Interestingly, Lin28b is preferentially expressed in fetal HSCs and was recently shown to be a major positive regulator of glucose metabolism (14). Thus, we hypothesized that metabolic changes between neonatal and adult CD8$^+$ T cells could be attributed to developmentally-related differences in Lin28b expression. To test this, we crossed gBT-I mice with Lin28b Tg mice to generate a source of adult donor CD8$^+$ T cells that expressed Lin28b. We then cotransferred an equal number of WT adult (Thy1.1) and Lin28b Tg adult (Thy1.2) donor CD8$^+$ T cells into the same recipient mice (Ly5.2) and asked whether forced expression of Lin28b in adult CD8$^+$ T cells drives a more "neonatal-like" metabolic program postinfection with LM-gB (Fig. 3A). Consistent with our previous work, we found that Lin28b Tg adult donor cells preferentially became SLECs during infection, similar to neonatal CD8$^+$ T cells (Fig. 3B). At 7 dpi, we sorted out WT and Lin28b Tg donor CD8$^+$ T cells and compared their metabolic profiles via extracellular flux analysis. Induction of Lin28b in adult CD8$^+$ T cells resulted in lower rates of cellular respiration and a decrease in SRC (Fig. 3C–E), levels similar to those observed in neonatal donor CD8$^+$ T cells (Fig. 2). The Lin28b Tg cells also displayed higher rates of glycolytic metabolism (Fig. 3F, 3G), suggesting that Lin28b promotes rapid differentiation of CD8$^+$ T cells in early life by enhancing glucose metabolism.

Inhibiting glycolytic metabolism restores the formation of neonatal memory CD8$^+$ T cells

Our data thus far indicate that increased glycolysis in neonatal CD8$^+$ T cells is associated with more rapid effector cell

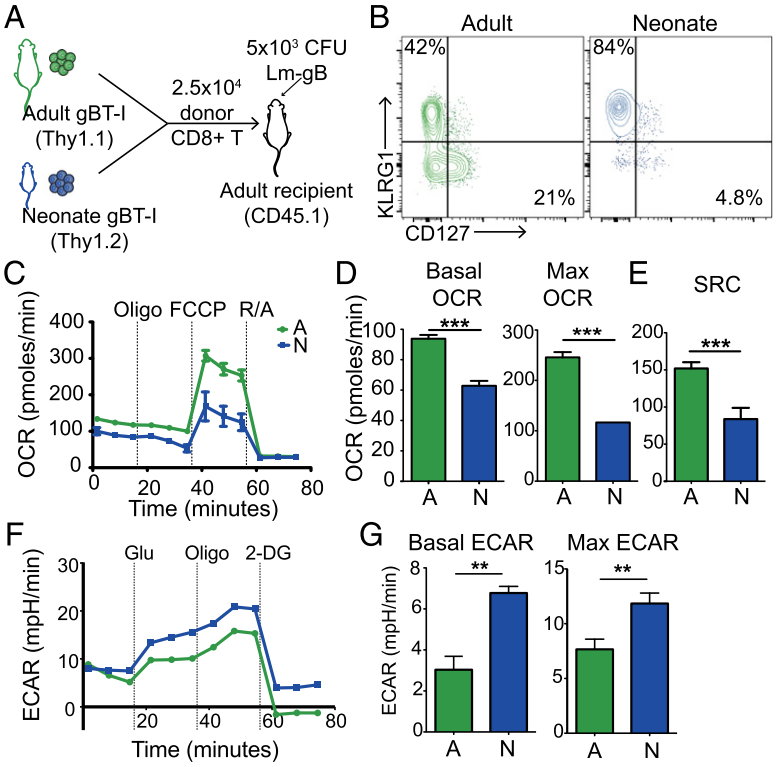

FIGURE 2. Neonatal CD8+ T cells possess an inherent propensity to undergo glycolytic metabolism following infection. (**A**) The experimental design to examine the metabolic programs of neonatal and adult CD8+ T cells during infection. (**B**) Representative contour plots of KLRG1 and CD127 expression at 7 dpi. (**C**) OCR measurements, (**D**) basal and maximum OCR, and (**E**) SRC values in adult and neonatal CD8+ T cells during a mitochondrial stress test at 7 dpi. (**F**) ECAR measurements and (**G**) basal and maximum ECAR values of adult and neonatal CD8+ T cells during a glycolysis stress test at 7 dpi. Data representative of two independent experiments with three biological replicates per group. $^{**}p < 0.005$, $^{***}p < 0.0005$ by unpaired Student *t* test.

differentiation. However, whether changes in glucose metabolism are ultimately responsible for altering the fate of neonatal CD8+ T cells during infection is unclear. Recent studies have demonstrated that CD8+ T cells with high glycolytic metabolism are short-lived and quickly die post-infection, whereas those with low glycolytic metabolism persist and transition into the long-lived memory pool (33). Thus, we hypothesized that neonatal CD8+ T cells are impaired at forming memory because they undergo a more pronounced glycolytic flux after antigenic stimulation. To test this hypothesis, we designed an experiment to limit glucose metabolism in neonatal CD8+ T cells before priming and examined changes in their ability to respond to infection. Our strategy involved stimulating neonatal and adult CD8+ T cells

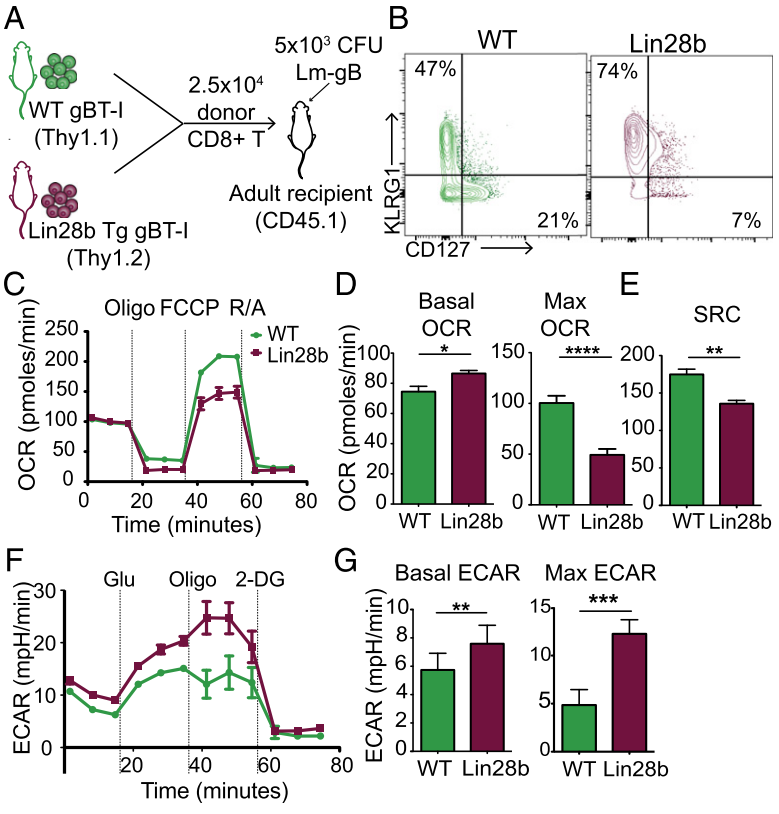

FIGURE 3. Lin28b drives a more glycolytic metabolic program in CD8+ T cells. (**A**) The experimental design to examine the metabolic programs of WT adult and Lin28b Tg adult CD8+ T cells during infection. (**B**) Representative contour plot of KLRG1 and CD127 expression at 7 dpi. (**C**) OCR measurements, (**D**) basal and maximum OCR, and (**E**) SRC values in adult and neonatal CD8+ T cells at 7 dpi from a mitochondrial stress test. (**F**) ECAR measurements and (**G**) basal and maximum ECAR values in WT and Lin28b Tg CD8+ T cells from a glycolysis stress test at 7 dpi. Data representative of two independent experiments with three biological replicates per group. $^{*}p < 0.05$, $^{**}p < 0.005$, $^{***}p < 0.0005$, $^{****}p < 0.000$ by unpaired Student *t* test.

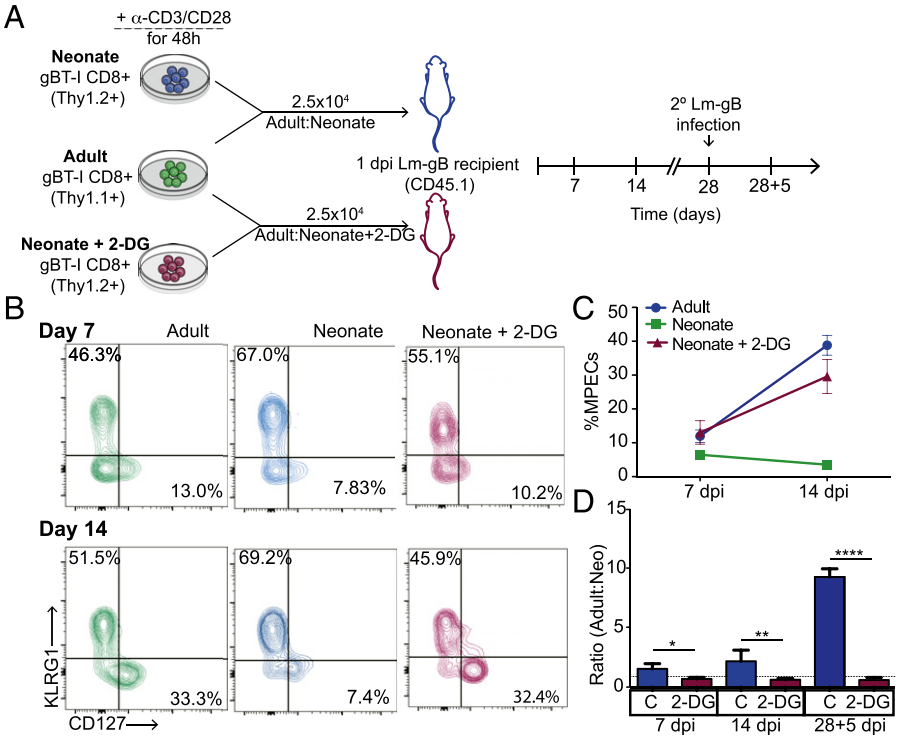

FIGURE 4. Inhibiting glycolytic metabolism restores the formation of neonatal memory CD8$^+$ T cells. (**A**) Schematic of the experimental design: adult and neonatal CD8$^+$ T cells were stimulated with anti-CD3 and anti-CD28 in the presence of a vehicle control or 0.3 mM 2-DG for 48 h. Then, 2.5×10^4 activated adult (Thy1.1) and neonatal (Thy1.2) cells were cotransferred i.v. into congenic WT recipients (CD45.1) that were infected with 5×10^3 CFU of LM-gB the previous day. Recipients were rechallenged with 5×10^4 CFU of LM-gB at 28 dpi. Phenotypes of donor cells were assessed through bleeds at indicated time points. (**B**) Representative contour plots of KLRG1 and CD127 expression at 7 and 14 dpi. (**C**) Percentage of adult, neonatal, and 2-DG neonatal cells that are MPECs at 7 and 14 dpi. (**D**) Ratio of adult and neonatal donor populations with respect to time. Data representative of three independent experiments with four to six biological replicates per group. $^*p < 0.05$, $^{**}p < 0.005$, $^{****}p < 0.00005$ by unpaired Student t test.

in vitro in the presence or absence of a competitive inhibitor for glucose (2-DG) and then cotransferring adult donor CD8$^+$ T cells with either neonatal (2-DG–treated) or neonatal (control) donor cells into an LM-gB–infected matched recipient (Fig. 4A). At various times postinfection, we examined the phenotype of each donor population and found that inhibiting glycolysis in neonatal cells resulted in significantly more MPECs and fewer SLECs (Fig. 4B, 4C). In fact, the neonatal cells treated with 2-DG exhibited a phenotype comparable to the adult donor CD8$^+$ T cells, indicating that a sizeable portion of 2-DG–treated cells were able to transition into the memory stage (Fig. 4B, 4C). Strikingly, 2-DG treatment also enabled neonatal CD8$^+$ T cells to survive during contraction and mount a more proliferative recall response following reinfection with LM-gB, similar to adult donor CD8$^+$ T cells (Fig. 4D). Thus, limiting entry into glycolysis is sufficient to limit terminal differentiation and promote the development of neonatal memory CD8$^+$ T cells.

In summary, these findings demonstrate that neonatal and adult CD8$^+$ T cells are intrinsically different and respond to Ag stimulation with dissimilar metabolic programs, leading them to adopt different fates. Higher glycolytic flux biases neonatal CD8$^+$ T cells to become short-lived effectors at the expense of forming memory cells. Perhaps counterintuitively, reducing glycolytic metabolism during priming can enhance the survival of neonatal memory CD8$^+$ T cells. These findings suggest that many of the intrinsic differences between neonatal and adult CD8$^+$ T cells can be attributed to age-related changes in metabolic reprogramming and demonstrate that neonatal memory T cell responses can be therapeutically enhanced.

Although the underlying basis for why neonatal and adult CD8$^+$ T cells use distinct metabolic programs requires further investigation, our findings suggest that neonatal CD8$^+$ T cells exhibit a different metabolic program than adults because they are derived from fetal-liver HSCs. Thus, it would be interesting to examine the metabolic programs in other fetal-derived lymphocytes to see if they also have a higher glycolytic flux than their adult counterparts. It is also interesting to speculate that Lin28b serves as a metabolic rheostat, balancing the need to generate different amounts of effector and memory cells at various stages of life. In the future, it will be important to investigate how the different metabolic states in neonatal and adult CD8$^+$ T cells influence their ability to give rise to different subsets of memory cells (e.g., tissue resident memory, central memory, and effector memory). Such studies could provide us with novel strategies to fine-tune the development of memory CD8$^+$ T cells during critical stages of development.

Disclosures

The authors have no financial conflicts of interest.

References

1. Chang, J., and T. J. Braciale. 2002. Respiratory syncytial virus infection suppresses lung CD8+ T-cell effector activity and peripheral CD8+ T-cell memory in the respiratory tract. *Nat. Med.* 8: 54–60.
2. Butz, E. A., and M. J. Bevan. 1998. Massive expansion of antigen-specific CD8+ T cells during an acute virus infection. *Immunity* 8: 167–175.
3. Doherty, P. C. 1998. The numbers game for virus-specific CD8+ T cells. *Science* 280: 227.
4. Murali-Krishna, K., J. D. Altman, M. Suresh, D. J. Sourdive, A. J. Zajac, J. D. Miller, J. Slansky, and R. Ahmed. 1998. Counting antigen-specific CD8 T cells: a reevaluation of bystander activation during viral infection. *Immunity* 8: 177–187.
5. Wissink, E. M., N. L. Smith, R. Spektor, B. D. Rudd, and A. Grimson. 2015. MicroRNAs and their targets are differentially regulated in adult and neonatal mouse CD8+ T cells. *Genetics* 201: 1017–1030.
6. Smith, N. L., E. Wissink, J. Wang, J. F. Pinello, M. P. Davenport, A. Grimson, and B. D. Rudd. 2014. Rapid proliferation and differentiation impairs the development of memory CD8+ T cells in early life. *J. Immunol.* 193: 177–184.
7. Reynaldi, A., N. L. Smith, T. E. Schlub, V. Venturi, B. D. Rudd, and M. P. Davenport. 2016. Modeling the dynamics of neonatal CD8$^+$ T-cell responses. *Immunol. Cell Biol.* 94: 838–848.
8. Wang, J., E. M. Wissink, N. B. Watson, N. L. Smith, A. Grimson, and B. D. Rudd. 2016. Fetal and adult progenitors give rise to unique populations of CD8+ T cells. *Blood* 128: 3073–3082.

9. Jotereau, F., F. Heuze, V. Salomon-Vie, and H. Gascan. 1987. Cell kinetics in the fetal mouse thymus: precursor cell input, proliferation, and emigration. *J. Immunol.* 138: 1026–1030.
10. Owen, J. J., and M. A. Ritter. 1969. Tissue interaction in the development of thymus lymphocytes. *J. Exp. Med.* 129: 431–442.
11. Foss, D. L., E. Donskoy, and I. Goldschneider. 2001. The importation of hematogenous precursors by the thymus is a gated phenomenon in normal adult mice. *J. Exp. Med.* 193: 365–374.
12. Shinoda, G., N. Shyh-Chang, T. Y. Soysa, H. Zhu, M. T. Seligson, S. P. Shah, N. Abo-Sido, A. Yabuuchi, J. P. Hagan, R. I. Gregory, et al. 2013. Fetal deficiency of lin28 programs life-long aberrations in growth and glucose metabolism. *Stem Cells* 31: 1563–1573.
13. Shyh-Chang, N., and G. Q. Daley. 2013. Lin28: primal regulator of growth and metabolism in stem cells. *Cell Stem Cell* 12: 395–406.
14. Zhu, H., N. Shyh-Chang, A. V. Segrè, G. Shinoda, S. P. Shah, W. S. Einhorn, A. Takeuchi, J. M. Engreitz, J. P. Hagan, M. G. Kharas, et al; MAGIC Investigators. 2011. The Lin28/let-7 axis regulates glucose metabolism. *Cell* 147: 81–94.
15. Thornton, J. E., and R. I. Gregory. 2012. How does Lin28 let-7 control development and disease? *Trends Cell Biol.* 22: 474–482.
16. Krauss, S., M. D. Brand, and F. Buttgereit. 2001. Signaling takes a breath--new quantitative perspectives on bioenergetics and signal transduction. *Immunity* 15: 497–502.
17. Rathmell, J. C., M. G. Vander Heiden, M. H. Harris, K. A. Frauwirth, and C. B. Thompson. 2000. In the absence of extrinsic signals, nutrient utilization by lymphocytes is insufficient to maintain either cell size or viability. *Mol. Cell* 6: 683–692.
18. Loos, J. A., and D. Roos. 1973. Changes in the carbohydrate metabolism of mitogenically stimulated human peripheral lymphocytes. 3. Stimulation by tuberculin and allogenic cells. *Exp. Cell Res.* 79: 136–142.
19. Warburg, O. 1956. On respiratory impairment in cancer cells. *Science* 124: 269–270.
20. Chang, C. H., J. D. Curtis, L. B. Maggi, Jr., B. Faubert, A. V. Villarino, D. O'Sullivan, S. C. Huang, G. J. van der Windt, J. Blagih, J. Qiu, et al. 2013. Posttranscriptional control of T cell effector function by aerobic glycolysis. *Cell* 153: 1239–1251.
21. Pearce, E. L., M. C. Walsh, P. J. Cejas, G. M. Harms, H. Shen, L. S. Wang, R. G. Jones, and Y. Choi. 2009. Enhancing CD8 T-cell memory by modulating fatty acid metabolism. *Nature* 460: 103–107.
22. Araki, K., A. P. Turner, V. O. Shaffer, S. Gangappa, S. A. Keller, M. F. Bachmann, C. P. Larsen, and R. Ahmed. 2009. mTOR regulates memory CD8 T-cell differentiation. *Nature* 460: 108–112.
23. van der Windt, G. J., and E. L. Pearce. 2012. Metabolic switching and fuel choice during T-cell differentiation and memory development. *Immunol. Rev.* 249: 27–42.
24. Mueller, S. N., W. Heath, J. D. McLain, F. R. Carbone, and C. M. Jones. 2002. Characterization of two TCR transgenic mouse lines specific for herpes simplex virus. *Immunol. Cell Biol.* 80: 156–163.
25. Pobezinsky, L. A., R. Etzensperger, S. Jeurling, A. Alag, T. Kadakia, T. M. McCaughtry, M. Y. Kimura, S. O. Sharrow, T. I. Guinter, L. Feigenbaum, and A. Singer. 2015. Let-7 microRNAs target the lineage-specific transcription factor PLZF to regulate terminal NKT cell differentiation and effector function. *Nat. Immunol.* 16: 517–524.
26. Wang, R., C. P. Dillon, L. Z. Shi, S. Milasta, R. Carter, D. Finkelstein, L. L. McCormick, P. Fitzgerald, H. Chi, J. Munger, and D. R. Green. 2011. The transcription factor Myc controls metabolic reprogramming upon T lymphocyte activation. *Immunity* 35: 871–882.
27. Liu, X., Z. Ser, and J. W. Locasale. 2014. Development and quantitative evaluation of a high-resolution metabolomics technology. *Anal. Chem.* 86: 2175–2184.
28. Smith, N. L., R. K. Patel, A. Reynaldi, J. K. Grenier, J. Wang, N. B. Watson, K. Nzingha, K. J. Yee Mon, S. A. Peng, A. Grimson, et al. 2018. Developmental origin governs CD8+ T cell fate decisions during infection. *Cell* 174: 117–130.e14.
29. Adkins, B., T. Williamson, P. Guevara, and Y. Bu. 2003. Murine neonatal lymphocytes show rapid early cell cycle entry and cell division. *J. Immunol.* 170: 4548–4556.
30. Palin, A. C., V. Ramachandran, S. Acharya, and D. B. Lewis. 2013. Human neonatal naive CD4+ T cells have enhanced activation-dependent signaling regulated by the microRNA miR-181a. *J. Immunol.* 190: 2682–2691.
31. Schönland, S. O., J. K. Zimmer, C. M. Lopez-Benitez, T. Widmann, K. D. Ramin, J. J. Goronzy, and C. M. Weyand. 2003. Homeostatic control of T-cell generation in neonates. *Blood* 102: 1428–1434.
32. van der Windt, G. J., B. Everts, C. H. Chang, J. D. Curtis, T. C. Freitas, E. Amiel, E. J. Pearce, and E. L. Pearce. 2012. Mitochondrial respiratory capacity is a critical regulator of CD8+ T cell memory development. *Immunity* 36: 68–78.
33. Sukumar, M., J. Liu, Y. Ji, M. Subramanian, J. G. Crompton, Z. Yu, R. Roychoudhuri, D. C. Palmer, P. Muranski, E. D. Karoly, et al. 2013. Inhibiting glycolytic metabolism enhances CD8+ T cell memory and antitumor function. *J. Clin. Invest.* 123: 4479–4488.